Radial Profiles of Lunar Basins. Charles J. Byrne, Image Again, 39 Brandywine Way, Middletown, NJ 07748, charles.byrne@verizon.net.

Introduction: The comprehensive coverage of the elevation data from the Clementine mission provides a tool for the analysis of lunar basin profiles. The radial profiles of seven basins were measured and (after normalization) an analytic model was generated for the set of profiles. The selected basins cover a wide range of sizes and locations and are relatively free of distortion by nearby features.

The motivation of this study was to investigate the dynamics of basin formation in support of a search for a basin or basins underlying the region of maria on the near side of the Moon {1].

Selected basins: The selected basins are Grimaldi, Humorum, Hertzsprung, Humboldtianum, Korolev, Moscoviense, and Orientale. Well distributed in latitude and longitude, they have varied characteristics, including partial mare flooding and no, one, or two internal rings.

Radial elevation profile: The elevation data source was Topogrd2 [2], derived from the measurements of the Clementine mission. For each basin, the data was transformed into circular coordinates with the center of each basin as the origin. After starting with parameters from photogeology [3], the latitude and longitude of the center [3] were adjusted (to 0.25 degrees) for the clearest elevation profile. An offset from the center reduces the detail in the profiles. For each radius in 0.25 degree increments the elevations were averaged over 360 degrees in azimuth As a result, odd azimuthal harmonics of the surface topography (such as tilt) were removed, leaving the central elevation, the circularly symmetric profile, cylindrical and spherical curvature, and higher order even terms. The resulting elevation profile of the Orientale Basin is shown in Figure 1.

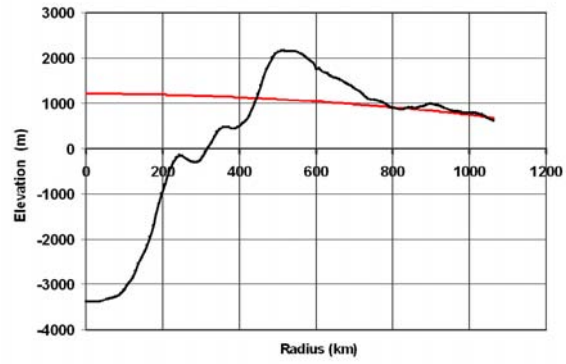

Figure 1: Radial elevation profile of the Orientale Basin. The elevations of Topogrd2 were averaged over 360 degrees of azimuth around a center at 19.5 South and 94.75 West. The red curved line represents the estimated correction for the central elevation and curvature.

Curvature correction: As mentioned, the elevation profile contains a component representing the cylindrical and spherical shapes of the surface, either characteristic of the target surface before impact, due to isostatic adjustment of the crust, or from subsequent impacts. As we shall see, the major source of this component appears to be isostatic adjustment. In any case, the central elevation and curvature adjustments are estimated, with criteria that the edge of the basin be at the point of maximum slope of the profile and that the depth of ejecta be very small for radii beyond 2.3 times the radius of the edge of the basin. Figure 1 shows the adjustment components for the Orientale Basin.

Radial depth profile: A depth profile, as shown in Figure 2, is independent of the topography of the target surface before impact and after isostatic adjustment.

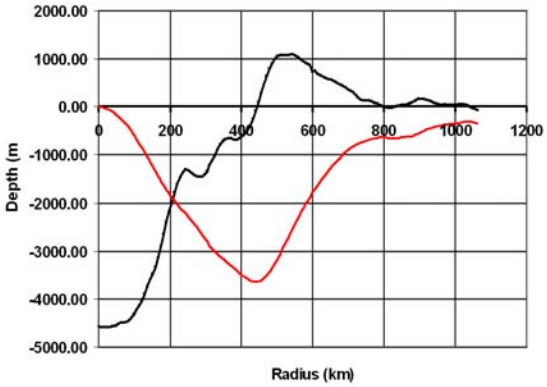

Figure 2: Radial depth profile of the Orientale Basin. The elevation and curvature estimations of Figure 1 have been subtracted. The radius of interception of the target surface, R_{IS}, is slightly smaller that the radius derived by photographic interpretation, which is likely to the radius of the cliffs of Cordillara Montes. The volume curve (Units are 4 times km^3) is derived by integration of the depth profile.

Depth profiles were derived fpr the rest of the selected basins. Parameters of the seven basins are shown in Table 1. The depth profiles are shown in Figure 3. The empirical profile is consistent with sand table and explosion data reported in [4].

Table 1

Basin	Center		Surface Adjustment	
	Latitude	Longitude	Elevation	Curvature
Grimaldi	-5.25	-68.50	-1050	-4.67
Hertzsprung	1.50	-129.50	3800	-1.89
Humboldtianum	57.75	82.50	-1600	0.03
Humorum	-24.50	-39.50	-2100	0.28
Korolev	-4.25	-157.50	4800	-5.56
Moscoviense	26.25	147.25	850	-0.61
Orientale	-19.50	-94.75	1200	-0.42

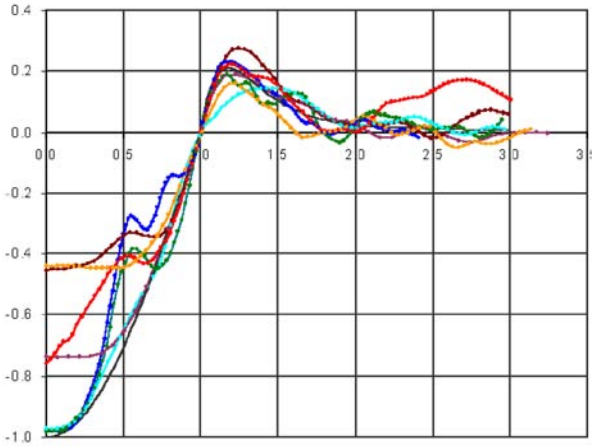

Figure 3: Depth profiles of the selected basins, normalized by both radius and depth, are superimposed. The black line is the empirical model that best represents the normalized profiles, neglecting internal rings, mare flooding, and external rings.

Vertical normalization: Assigning a value to the central depth of the original basin is easy for Grimaldi, Moscoviense, or Orientale which have only a little mare flooding. However for those with heavy flooding there is strong reliance on the slope of the basin just inside of the rim, which is exposed above the mare. Consideration of the volume budget is also helpful.

Empirical model: The internal basin is modeled by a negative cosine curve: $Z'(r') = -Cos(r'\pi/2)$

For $0 \le r' \le 1$

Where Z(r') is the depth

r' is the internal normalized radius

The internal shape of a basin is sometimes described as a parabola, but the cosine function is a better fit to these basins, especially for the slope near the surface intercept.

The external ejecta has three segments, the rounded rim, the far field, and a transition region between them. All three segments are modeled by the following equation:

$$Z'(R') = 3.0(R'-1)e^{-(R'-1)/0.166} + Z'_{FF}(R'^{-3} - R'^{-4})$$

For R' > 1 (the external radius)

Where Z'_{FF}, the normalized far field coefficient, is 0.30 for no internal rings, 0.20 for only an inner ring, or 0.15 for an intermediate ring as well.

The far field depth approaches an inverse cube of the radius [4]. The presence of internal rings above the negative cosine curve reduces the volume ejected from the basin. Since there is no evidence of volume being missing from the rounded rim or ejecta blanket, the far field ejecta must be reduced as described above.

Inner rings: Inner rings are modeled by adding a raised cosine function to the negative cosine function. For basins with one inner ring, the following equation is a good fit:

$$Z'(r') = 0.33 \bullet 0.5\{1 + Cos[2(r'-0.5)2\pi]\}$$

For $0.25 \le r' \le 0.75$

Isostatic adjustment: The curvature adjustment illustrated in Figure 1 and listed in Table 1 is negative for a buldge and positive for a depression. Bulges may be due to isostatic adjustment; an upwelling of material to compensate for the material ejected from the internal basin. Only a few of the selected basins show large curvature corrections, and large corrections are always bulges. Figure 4 shows how curvature corrections relate to the latitudes of basin centers. Clearly, basins near the equator show much more mounding (presumably isostatic adjustment) than basins that are nearer the poles. A possible reason for this is that the crust and upper mantle were more plastic near the equator, warmed by the greater tidal forces exerted by Earth's gravity there. Although other mechanisms of modification have been suggested [3], the evidence of this new approach should also be considered.

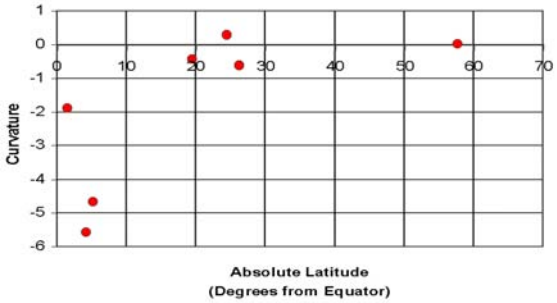

Figure 4: Curvature correction of each of the seven basins plotted against their absolute latitude (distance from the equator). Only the three basins within 10 degrees of the equator show negative curvature corrections greater than 0.5 m/degree^2, a sign of isostatic adjustment.

Summary: Doubly normalized elevation profiles have been corrected to depth profiles and compared. An empirical analytic model has been constructed that fits the basins, including their internal rings, mare flooding, and ejecta but excluding their external rings. A new type of evidence concerning isostatic adjustment has been presented. Additional basins, both named and unnamed, meet the selection criterion and should be analyzed by this method to improve the statistics. An algorithm that detects arcs would improve the quality of the data on rings.

References: [1] Byrne, C. J., 2006, The Near Side Megabasin of the Moon, submitted to LPSC 2006. [2]] Zuber, M. T., et al., 2004, Topogrd1 and Topogrd2, web site of the University of Washington at St. Louis, http://wufs.wustl.edu/geodata/clem1-gravity-topo-vl/. [3] Spudis, P. D., 1993, The Geology of Multi-Ring Impact Basins, Cambridge University Press. [4] Housen, K. R. et al., 1983, Crater Ejecta Scaling Laws, JGR, 88.